



## A Comparison of the Bidomain and EMI Models in Refractory Cardiac Tissue

Joyce Reimer<sup>1</sup>    Sebastián A. Domínguez-Rivera<sup>2</sup>  
Joakim Sundnes<sup>3</sup>    Raymond J. Spiteri<sup>4</sup>

<sup>1</sup>Division of Biomedical Engineering    <sup>2</sup>Department of Mathematics and Statistics,  
<sup>3</sup>Simula Research Laboratory, Oslo, Norway,    <sup>4</sup>Department of Computer Science



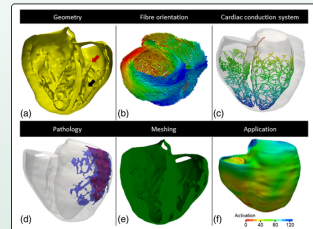
Go20 Conference 2023

# Outline

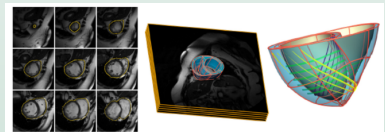
- 1 Background
  - Cardiac Modelling
  - Motivation
- 2 Methods
  - Mathematical Models
  - Experimental Protocol
  - Solving Methods
- 3 Results
  - S1-S2 Experiments
  - Strength-Interval Curves
- 4 Discussion
  - Differences Between Models
  - Limitations & Future Work
  - Summary

# State of Cardiac Modelling

- Computational cardiac models are becoming more feasible for routine clinical use
  - Precision ablations
  - Mapping of heart from ECGs
  - Arrhythmia risk assessment
- Heart has 2-3 billion myocardial cells (~10 billion cells total)
  - heavy computational demands
  - trade-off between physiological accuracy and clinical feasibility



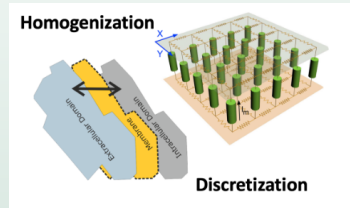
(Niederer et al., 2009)



(Lopez-Perez et al., 2015)

# Bidomain Model

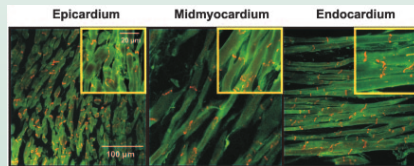
- Most cardiac modelling employs the bidomain or monodomain models
- Bidomain model is based on a volume-averaging approach of electrical activity in cardiac cells
- Monodomain model is a reduced formulation of the bidomain model



(Computational Cardiology Lab)

# Limitations of Conventional Models

- The bidomain and monodomain models treat cells homogeneously as a continuum
- An insufficient assumption when discontinuities at the cellular level are implicated in a certain disease or phenomenon
- To address these models' limitations, the extracellular-membrane-intracellular (EMI) model was developed by Tveito et al. in 2017



(Glukhov et al., 2010)

# Bidomain Model

$$\chi C_m \frac{\partial v}{\partial t} + \chi I_{ion}(v, \mathbf{s}) = \nabla \cdot (\sigma_i \nabla v) + \nabla \cdot (\sigma_i \nabla u_e),$$
$$0 = \nabla \cdot (\sigma_i \nabla v) + \nabla \cdot ((\sigma_i + \sigma_e) \nabla u_e),$$

subject to

$$0 = \hat{\mathbf{n}} \cdot (\sigma_i \nabla v + \sigma_i \nabla u_e),$$

$$0 = \hat{\mathbf{n}} \cdot (\sigma_e \nabla u_e),$$

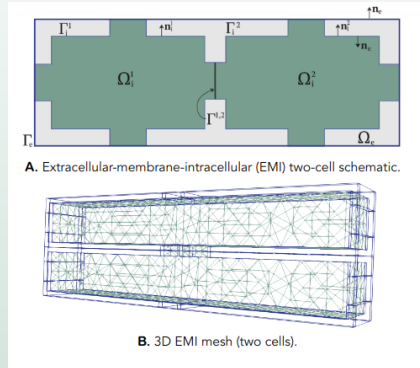
and initial conditions.

# Extracellular-Membrane-Intracellular (EMI) Model

$$\begin{aligned}
 -\nabla \cdot (\sigma_e \nabla u_e) &= 0, \quad \text{in } \Omega_e, \\
 -\nabla \cdot (\sigma_i^{(k)} \nabla u_i^{(k)}) &= 0, \quad \text{in } \Omega_i^{(k)}, \quad k = 1, 2, \\
 \frac{\partial v^{(k)}}{\partial t} &= \frac{1}{C_m^{(k)}} (I_m^{(k)} - I_{ion}^{(k)}), \quad \text{on } \Gamma_i^{(k)}, \\
 \frac{\partial w}{\partial t} &= \frac{1}{C^{(1,2)}} (I^{(1,2)} - I_{gap}), \quad \text{on } \Gamma^{(1,2)},
 \end{aligned}$$

where

$$\begin{aligned}
 v^{(k)} &= u_i^{(k)} - u_e, \quad \text{on } \Gamma_i^{(k)}, \quad k = 1, 2, \quad \text{and} \\
 w &= u_i^{(1)} - u_i^{(2)}, \quad \text{on } \Gamma^{(1,2)}.
 \end{aligned}$$



# Extracellular-Membrane-Intracellular (EMI) Model

## Boundary and Flux Conditions:

$$u_e = 0, \quad \text{on } \Gamma_e,$$

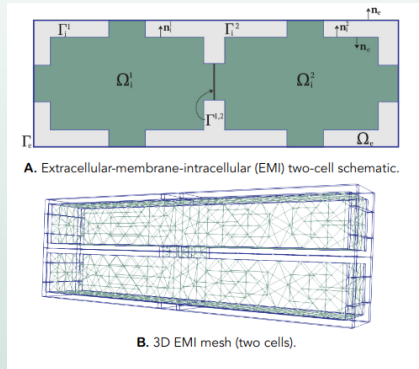
$$(\sigma_e \nabla u_e) \cdot \hat{\mathbf{n}}_e^{(k)} = -(\sigma_i^{(k)} \nabla u_i^{(k)}) \cdot \hat{\mathbf{n}}_i^{(k)}, \quad \text{on } \Gamma_i^{(k)},$$

$$k = 1, 2,$$

$$(\sigma_i^{(2)} \nabla u_i^{(2)}) \cdot \hat{\mathbf{n}}_i^{(2)} = -(\sigma_i^{(1)} \nabla u_i^{(1)}) \cdot \hat{\mathbf{n}}_i^{(1)}, \quad \text{on } \Gamma^{(1,2)}.$$

$$I_m^{(k)} = -(\sigma_i^{(k)} \nabla u_i^{(k)}) \cdot \hat{\mathbf{n}}_i^{(k)}, \quad \text{on } \Gamma_i^{(k)}, k = 1, 2,$$

$$I^{(1,2)} = -(\sigma_i^{(1)} \nabla u_i^{(1)}) \cdot \hat{\mathbf{n}}_i^{(1)}, \quad \text{on } \Gamma^{(1,2)}.$$



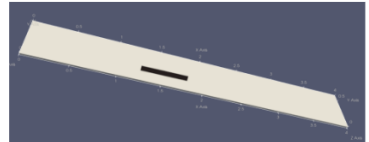
# Aims of Study

In this study, we:

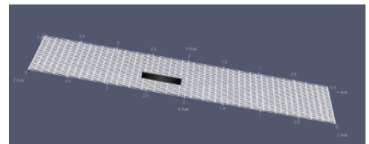
- Carry out a comparison study between the bidomain and EMI models in the area of tissue refractoriness
- Search for the threshold currents required to stimulate consecutive APs separated by varying time intervals and plot these on strength-interval curves
- Compare the curves from each model against experimental data to identify differences and evaluate accuracy

# Simulation Domain

- Tissue size:  $4 \text{ mm} \times 0.625 \text{ mm} \times 0.025 \text{ mm}$  (625 cells,  $25 \times 25 \times 1$ )
- Electrode dimensions:  $0.5 \text{ mm} \times 0.1 \text{ mm} \times 0.025 \text{ mm}$ , positioned in bottom third of domain (one electrode = unipolar)
- All currents delivered via an initial transmembrane stimulus in the cell model

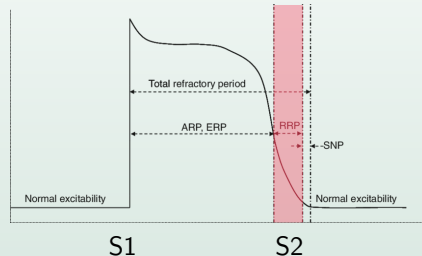
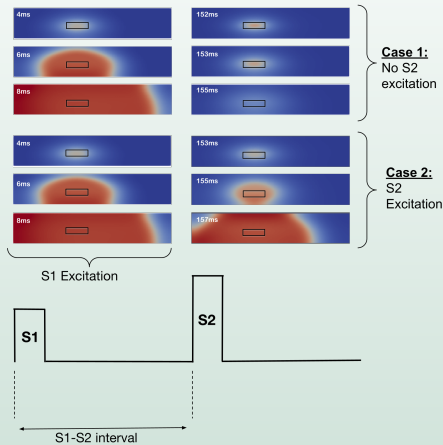


A. Bidomain computational domain.



B. EMI computational domain.

# S1-S2 Stimulus Protocol



ARP = Absolute Refractory Period  
 RRP = Relative Refractory Period  
 (Jaye et al., 2010)

# Numerical and Programming Methods

- Cell model: Gray and Pathmanathan's 2016 parsimonious ionic model based on rabbit action potentials
- Time evolution with first order Godunov operator splitting
  - Cell model (ODE) solver: Forward Euler or Rush–Larsen
  - PDE Solver: Backward Euler
- Spatial discretization with Finite Element Method
- Software implementation:
  - Bidomain: Modified Chaste (Pitt-Francis et al., 2009)
  - EMI: FreeFEM++ (Hecht et al., 2012)

# Parameters

Table: Bidomain parameters.

Parameter	Value
$\sigma_{i,x}$	$0.2525 \mu\text{A mV}^{-1}\text{mm}^{-1}$
$\sigma_{i,y}$	$0.0222 \mu\text{A mV}^{-1}\text{mm}^{-1}$
$\sigma_{i,z}$	$0.0222 \mu\text{A mV}^{-1}\text{mm}^{-1}$
$\sigma_{e,x}$	$0.821 \mu\text{A mV}^{-1}\text{mm}^{-1}$
$\sigma_{e,y}$	$0.215 \mu\text{A mV}^{-1}\text{mm}^{-1}$
$\sigma_{e,z}$	$0.215 \mu\text{A mV}^{-1}\text{mm}^{-1}$
$C_m$	$0.01 \mu\text{F mm}^{-2}$
$\chi$	$150 \text{ mm}^{-1}$
$\Delta x$	$0.025 \text{ mm}$

Table: EMI parameters.

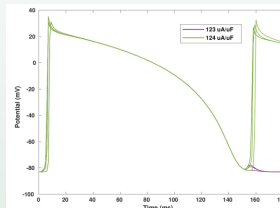
Parameter	Value
$\sigma_i$	$0.5 \mu\text{A mV}^{-1}\text{mm}^{-1}$
$\sigma_e$	$2.0 \mu\text{A mV}^{-1}\text{mm}^{-1}$
$C_m, C^{(k,l)}$	$0.01 \mu\text{F mm}^{-2}$
$R^{(k,l)}$	$0.15 \text{ mV}\cdot\text{mm}^2\mu\text{A}^{-1}$
$\Delta x$	$0.005 \text{ mm}$

- The bidomain conductivities,  $\sigma$ , are calibrated values.
- The bidomain surface-to-volume-ratio,  $\chi$ , is derived from the structure of the EMI domain.

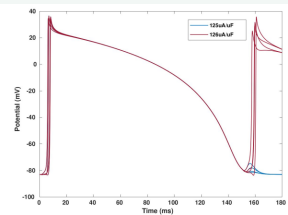
# S1-S2 Experiments: Action Potential Traces

## Action Potentials:

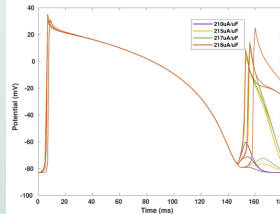
- The S2 thresholds of each interval can be identified by plotting the potentials at different points across the domain



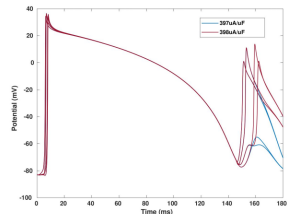
A. Bidomain AP Traces, S2 at 150 ms.



B. EMI AP Traces, S2 at 150 ms.



C. Bidomain AP Traces, S2 at 145 ms.

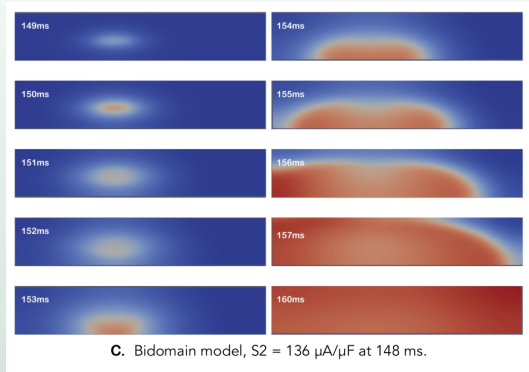


D. EMI AP Traces, S2 at 145 ms.

# S1-S2 Experiments: Domain Visualization

## Domain Visualization:

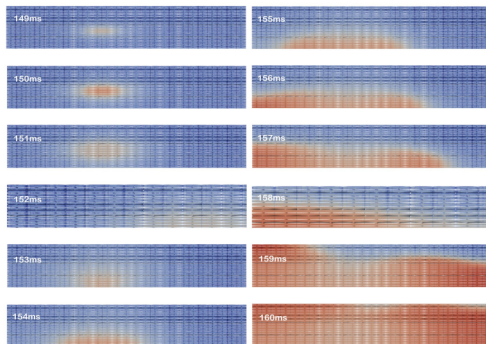
- S2 thresholds can also be determined by looking at time-lapse images of the domains



# S1-S2 Experiments: Domain Visualization

## Domain Visualization:

- S2 thresholds can also be determined by looking at time-lapse images of the domains

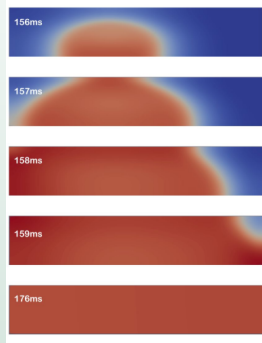


D. EMI model,  $S_2 = 162 \mu\text{A}/\mu\text{F}$  at 148 ms.

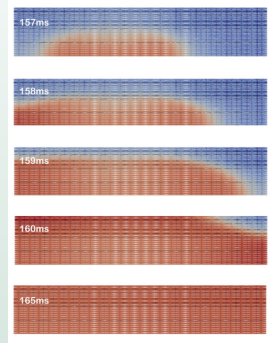
# S1-S2 Experiments: Domain Visualization

## Domain Visualization:

- Other information about the degree of refractoriness can be determined by looking at the mechanism of excitation (i.e., make vs. break)



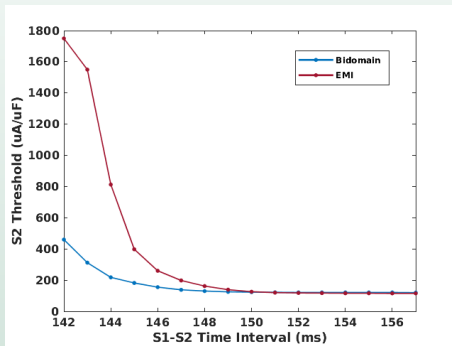
Make (bidomain, S2 at 150 ms)



Break (EMI, S2 at 150 ms)

# Strength-Interval Curves: Bidomain and EMI

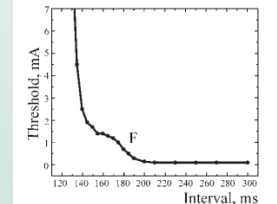
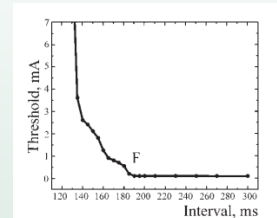
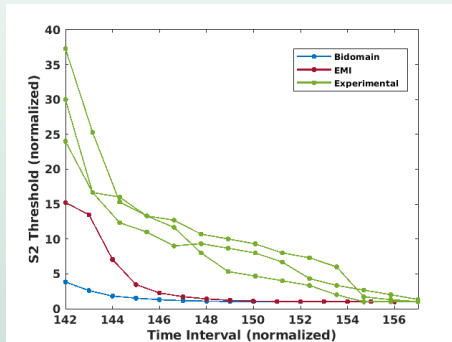
## The Bidomain and EMI Strength-Interval Curves:



# Differences Between Models

## Shape of the SI Curve:

- The EMI model's strength-interval curve is closer to experimental data

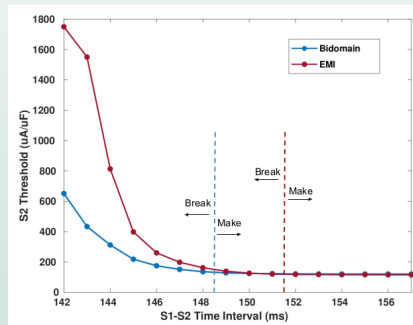


Experimental data from Sidorov et al., 2005

# Differences Between Models

## The Relative Refractory Period:

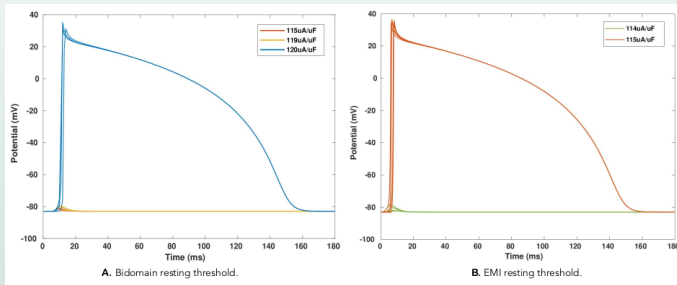
- EMI's RRP is longer and more accurate than the bidomain model:



# Differences Between Models

## The Resting Threshold:

- EMI's resting threshold is lower than the bidomain model's



# Limitations & Future Work

## Study Limitations & Future Work:

- Calibration parameter search was limited to the bidomain conductivities
- Small computational domain relative to experimental data on whole heart due to long computation time of EMI model
  - Parallelized EMI code is needed
- Electrodes were modelled via transmembrane stimulus.
  - A comparison of other electrode modelling methods needed (e.g. boundary conditions)

## Summary of Findings

- Our results show that there is a difference between the bidomain and EMI representations of the cardiac refractory period
- The results show that the EMI model outperforms the bidomain in representing physiological data in this area
- Other differences between models include
  - The rheobase value: EMI's is lower than bidomain
  - The length of the RRP: EMI's is longer than the bidomain

# References



Domínguez, S., Reimer, J., Green, K.R., Zolfaghari, R., Spiteri, R.J.  
A simulation-based method to study the LQT1 syndrome remotely using the EMI model.  
*Emerging Technologies in Biomedical Engineering and Sustainable TeleMedicine*, 179–189 (2021).



Galappathige, S.K., Gray, R.A., Roth, B.J.  
Cardiac strength-interval curves calculated using a bidomain tissue with a parsimonious ionic current.  
*PLoS ONE*, 12(2), e0171144 (2017).



Schalij, M.J., Lammers, W.J.E.P., Rensma, P.L., Allesie, M.A.  
Anisotropic in perfused conduction epicardium and reentry of rabbit left ventricle.  
*Am J Physiol Heart Circ Physiol*, 263(5), H1466–H1478 (1992).



Sidorov, V.Y., Woods, M.C., Baudenacher, P., Baudenbacher, F.  
Examination of stimulation mechanism and strength-interval curve in cardiac tissue.  
*Am J Physiol Heart Circ Physiol*, 289, H2602–H2615 (2005).



Tveito, A., Jaeger, K.H., Kuchta, M., Mardal, K.A., Rognes, M.E.  
A cell-based framework for numerical modeling of electrical conduction in cardiac tissue.  
*Frontiers in Physics*, 5(Oct), 1-18 (2017).